

## A new polarized target for structure studies on biomolecules at GKSS

M. Hirai<sup>1</sup>, W. Knop<sup>2</sup>, H.-J. Schink<sup>2</sup>, H.B. Stuhrmann<sup>2</sup>, R. Wagner<sup>2</sup>, J. Zhao<sup>2</sup>, O. Schärpf<sup>3</sup>, R.R. Crichton<sup>4</sup>, M. Krumpole<sup>5</sup>, K. Nierhaus<sup>6</sup>, T.O. Niinikoski<sup>7</sup> and A. Rijllart<sup>7</sup>

1 Kanagawa Inst. Technology, Atsugi-shi, Kanagawa-ken 243-02, Japan

2 GKSS Forschungszentrum, D-2054 Geesthacht, Germany

3 Inst. Laue Langevin, F-38042 Grenoble, France

4 Unité de Biochimie, Université Catholique de Louvain, B-1318 Louvain-la-Neuve

5 Department of Chemistry, University of Illinois, Chicago, USA

6 Max-Planck-Inst. für Molekulare Genetik, Berlin, Germany

7 CERN-EP, Geneva, Switzerland

### ABSTRACT

The Small-Angle Neutron Scattering instrument (SANS-1) which has been designed for the fields of molecular biology and polymer research has been put into operation in the new experimental hall for neutron scattering at the research reactor FRG-1 equipped with a Cold Neutron Source and a beryllium reflector at the GKSS Research Center. SANS-1 has been equipped with a polarized target station for the measurement of polarized neutron scatterings, which is mainly dedicated to the use of nuclear spin contrast variation method. The nuclear spins of protons and deuterons in most polymers and biological macromolecules can be almost aligned by dynamic nuclear polarization (DNP) with respect to an external magnetic field of 2.5 tesla at temperatures below 1 K in the presence of paramagnetic centers via 4 mm microwave irradiation, where one of them can be depolarized selectively by irradiation of their proper nuclear resonance frequency. First experiments using SANS-1 have been carried out with apoferritin and deuterated large subunit of E.coli ribosomes.

### I. INTRODUCTION

During the last three years, a Cold Neutron Source using  $\text{GH}_2$  with 1.5 kW cooling power has been installed in the research reactor FRG-1 (5MW light water swimming-pool reactor). At the same time, new experimental facilities for neutron scattering have been constructed in the enlarged new experimental hall. This hall has five cold neutron guides and eleven spectrometers one third of which utilize polarized neutrons. One of the

small-angle scattering spectrometer, SANS-1, has been equipped with a polarized target station.

The first measurements of the scattering of polarized proton spin clusters of various proteins in deuterated medium confirmed the predicted concept of the nuclear spin contrast variation method in macromolecular structure research (Knop et al., 1986,1989). First experiments using SANS-1 has shown the feasibility of this method owing to the increase of the gain in neutron scattering by a factor of  $10^3$  compared to earlier experiments. A more detailed report of this study will be published (Knop et al.).

## II. METHOD

### II-1 Concept of spin contrast variation

Spin contrast variation is a most convenient method for in site structure determination. This method is a kind of isotopic label method using the dependency of scattering amplitude on the nuclear spin polarization. At first we will summarize its concept (Stuhrmann et al., 1986, Boulin et al., 1988).

The interest in polarized targets is due to the spin-dependent neutron scattering showed by Abragam et al. (1982). The Fermi scattering amplitude operator for a free nucleus is given by

$$a = b + 2BI \cdot s \quad \dots\dots (1)$$

where  $s$  and  $I$  are the spin operators of the neutron and the nucleus, respectively. The constants  $b$  and  $B$  are expressed as a function of the two eigenvalues  $b_+$  and  $b_-$  which correspond to the two different coupling channels  $I+1/2$  and  $I-1/2$ .

$$b = [(I+1)b_+ + Ib_-] / (2I + 1), \quad B = (b_+ - b_-) / (2I + 1) \quad \dots\dots (2)$$

When we assume that neutrons impinge on a collection of scattering centers at position  $r_i$  and that the nuclear spins have a polarization  $P$  with no correlation and that neutrons have a polarization  $P_n$  parallel to that of the nuclei, neutron differential cross section of this cluster is given by the following expression (Abragam and Goldmann, 1982):

$$\begin{aligned} d\sigma/d\Omega &= \sum_i \langle |a_i|^2 \rangle + \sum_{i \neq j} \langle a_i a_j^* \exp[-iQ \cdot (r_i - r_j)] \rangle \\ &= \sum_i [\langle |a_i|^2 \rangle - \langle a_i a_j \rangle_{i \neq j}] + \langle a_i a_j^* \rangle_{i \neq j} \sum_{ij} \exp[-iQ \cdot (r_i - r_j)] \\ &= (d\sigma/d\Omega)_{inc.} + (d\sigma/d\Omega)_{coh.} \end{aligned}$$

whence

$$(d\sigma/d\Omega)_{inc.} = \sum_i B_i^2 [I_i(I_i + 1) - P_n P_i I_i - P_i^2 I_i^2] \quad \dots\dots (3)$$

$$(\frac{d\sigma}{d\Omega})_{coh.} = |U(Q)|^2 + 2P_n \text{Re}[U(Q)V(Q)] + |V(Q)|^2 \quad \dots\dots (4)$$

where  $\langle \rangle$  means the spin variable average in the target,  $Q$  is the momentum transfer,  $U(Q)$  and  $V(Q)$  are the coherent scattering amplitudes obtained by the Fourier transforms of the invariant part  $u(r)$  and the polarization-dependent part  $v(r)$ , respectively. These terms are defined as

$$U(Q) = \sum_i b_i \exp(-iQ \cdot r_i) = F \{ \sum_i b_i \delta(r - r_i) \} = F \{ u(r) \} \quad \dots\dots (5)$$

$$V(Q) = \sum_i B_i I_i P_i \exp(-iQ \cdot r_i) = F \{ \sum_i B_i I_i P_i \delta(r - r_i) \} = F \{ v(r) \} \quad \dots\dots (6)$$

Under the conditions that the cluster with no preferred orientation has only one nuclear species with non zero spin, the coherent scattering intensity per cluster can be obtained as follows.

$$I(Q) = \langle |U(Q)|^2 \rangle + 2P_n \langle \text{Re}[U(Q)V(Q)] \rangle + \langle |V(Q)|^2 \rangle$$

$$\equiv I_u(Q) + P_n P I_{uv}(Q) + P^2 I_v(Q) \quad \dots\dots (7)$$

where  $\langle \rangle$  means the average of scattering intensity in momentum space. According to Eq. (7) it is clear that each of the basic scattering functions,  $I_u(Q)$ ,  $I_{uv}(Q)$  and  $I_v(Q)$ , can be obtained easily by a series of measurements of  $I(Q)$  at different  $P$  and  $P_n$ , that is,  $I_u(Q)$  from  $P = 0$ ,  $I_{uv}(Q)$  from the difference between  $P_n P = 1$  and  $-1$ ,  $I_v(Q)$  from the sum of  $P_n P = 1$  and  $-1$ .

In the case of small-angle scatterings from the dissolved molecules in the solvent with a mean scattering amplitude density  $\text{solvent} \bar{\rho}_u + \text{solvent} \bar{\rho}_v$ , the use of the definition of the scattering density is more convenient. So we can get the reformulation of Eq. (7) for  $P_n=1$  at zero angle as follows.

$$I(0) = V^2 [\bar{\rho}_u^2 + 2(\bar{\rho}_u \bar{\rho}_v) + \bar{\rho}_v^2] = V^2 (\bar{\rho}_u + \bar{\rho}_v)^2$$

$$= V^2 (\bar{\rho}_u + P \bar{\rho}'_v)^2 \equiv V^2 \bar{\rho}^2 \quad \dots\dots (8)$$

where  $V$  is the volume of the particle,  $\bar{\rho}_u$  and  $\bar{\rho}_v$  are the mean excess scattering densities with respect to the solvent per unit volume, which correspond to the invariant and polarization-dependent parts, respectively. Here  $\bar{\rho}$ ,  $\bar{\rho}_u$  and  $\bar{\rho}_v$  are termed so-called contrast of the whole cluster, isotope contrast and nuclear spin contrast, respectively. Those notations are defined in the same manner as is well-known isotope contrast variation method.

$$\bar{\rho}_u \equiv \sum b_i / V - \text{solvent} \bar{\rho}_u, \quad \bar{\rho}_v \equiv NBIP / V - \text{solvent} \bar{\rho}_v \equiv P \bar{\rho}'_v \quad \dots\dots (9)$$

$N$  is the number of atoms in the cluster which have a nuclear spin-dependent scattering amplitude.

## II-2 Dynamic polarization and selective depolarization

In the presence of paramagnetic centers, as which we used sodium bis(2-ethyl-2-hydroxybutyrate)oxochromate(V) monohydrate (abbreviated EHBA-Cr(V): Krumpolc et al., 1985), the nuclear spins of protons and deuteron in macromolecules can be polarized by the use of dynamic polarization method (Abragam and Goldmann, 1982). The polarizations  $P_H$ ,  $P_D$  and the spin temperatures  $T_H$ ,  $T_D$  are related by Brillouin functions:

$$P_H = \tanh(h\nu_H / 2kT_H) \quad \dots\dots (10)$$

$$P_D = 4\tanh(h\nu_D / 2kT_D) / (3 + \tanh^2(h\nu_D / 2kT_D)) \quad \dots\dots (11)$$

where  $\nu_H$  and  $\nu_D$  are the Larmor frequencies of protons and deuterons, respectively. Assuming equal-spin-temperature,  $T_H = T_D$ , a unique temperature  $T$  can substitute for the different temperatures. After a high steady state of the nuclear spin polarizations is attained by microwave injection, one of the spins, protons or deuterons, is saturated by suppling RF of  $\nu_H$  or  $\nu_D$ , instead of microwave. In order to attain a high steady state, the temperature must be reached as low as possible. For this purpose the concentration of Cr(V) complex must be also controlled to reduce dipole-dipole interaction in paramagnetic electrons and to have a appropriate dipole-dipole interaction between nucleus and paramagnetic electron, simultaneously.

Following simulated results, Fig.1-5, base on equal-spin-temperature hypothesis of two different spin systems, i.e., proton spin system and deuteron spin one at thermal contact. Fig. 1 and 2 show the dependencies of deuteron polarization and of

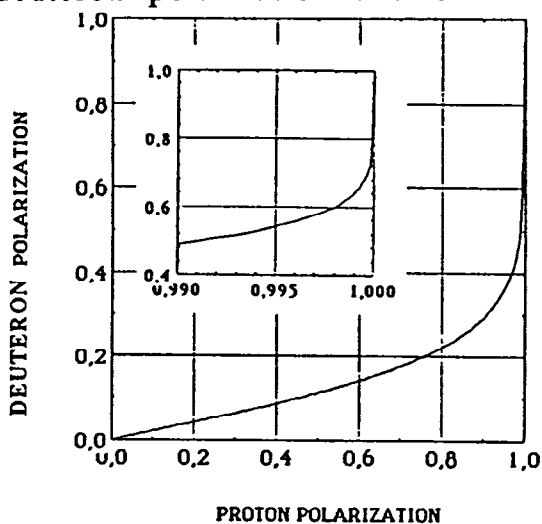
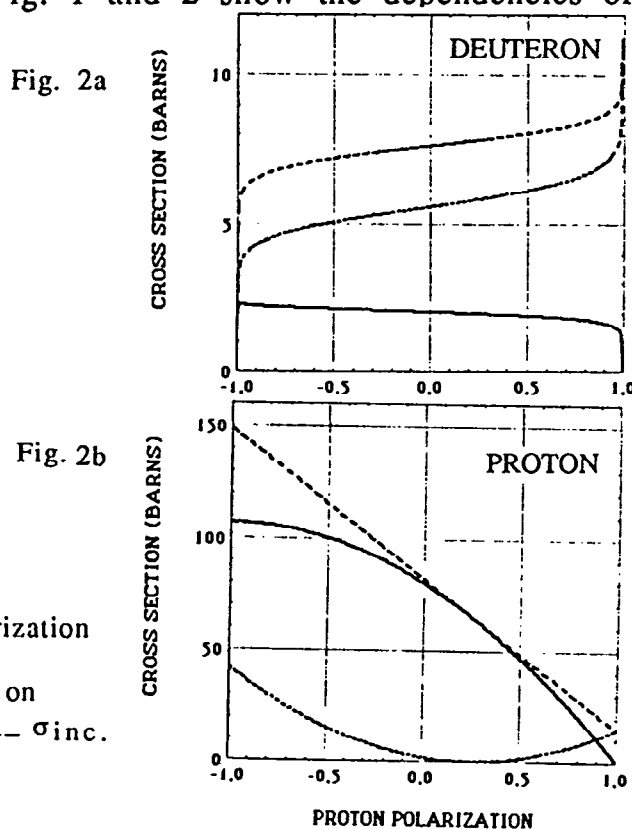


Fig. 1 Deuteron polarization vs. proton polarization

Fig. 2a & 2b The dependency of cross section on proton polarization: ----  $\sigma_{total}$ , ..... $\sigma_{coh.}$ , ---  $\sigma_{inc.}$



scattering cross sections on proton polarization (at  $P_N = 1$ ). In Fig. 3 we see how great experimental improvement for signal to noise ratio defined by (zero scattering int.)/(incoherent back ground scattering int.). In Fig. 4 and 5 (at  $P_N = 1$ ) so-called contrast is given by the difference between solvent and solute scattering densities. A contrast matching proton polarization is obtained from a point of intersection of both lines. For each simulation corresponding to Fig. 2-5, the concentration of solute is 2 wt% Urease and the deuteration ratios of solute, glycerol & water are 0%, 98.5% & 99.5%, respectively. The effect of H-D exchange is also considered.

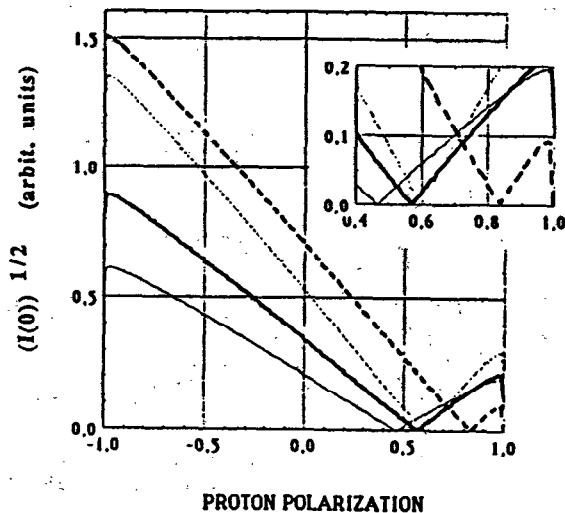


Fig. 4 Zero angle scattering int. vs. proton polarization: — protein, --- DNA, -.- lipid head, ..... lipid alkyl.

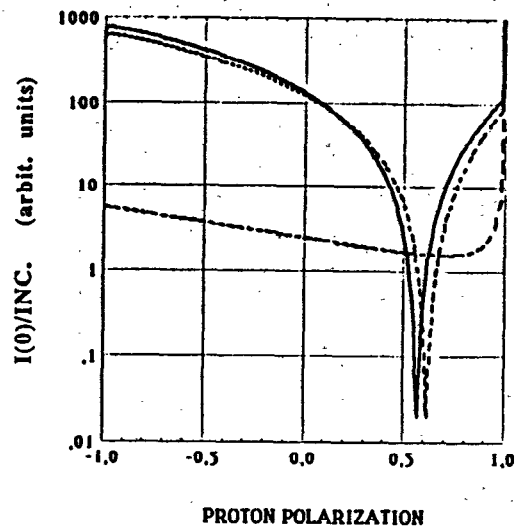


Fig. 5 Signal to Noise ratio of solution : — in  $D_2O$ , --- in  $H_2O$ , ..... in  $D_2O + D$ -glycerol (1:1).

### III. EXPERIMENTAL

#### III-1 Materials

Apo ferritin was prepared from horse spleen ferritin by the method described elsewhere (Jin and Crichton, 1987). This sample solution which contained 1.7 wt% apoferritin, 53 wt% deuterated glycerol, 45 wt%  $D_2O$ , 0.72 wt% EHBA ( $1.2 \times 10^{19}/cm^3$ ) and 2 wt%  $H_2O$  was quenched rapidly in a copper block cooled by liquid nitrogen and formed the frozen sample with the dimensions  $17 \times 17 \times 2 \text{ mm}^3$ .

The sample solution of deuterated large subunit of E.coli ribosomes contained 0.55 wt% subunit and almost the same amounts of other components as the apoferritin sample had. After quenching treatment was also same. The deuteration ratio of the subunit, 83%, was deduced from zero-angle scattering intensities. At this deuteration ratio, the scattering amplitude density of the subunit (at  $P=0$ ) is slightly more than half of that of the solvent. For sample preparation the rapid quenching and the existence of glycerol in solution is so important that we can eliminate the effect on solute molecular structure caused by the precipitation of water crystallites.

In the sample cell, two pieces of the frozen samples were aligned perpendicular to incident neutrons with the effective sample path length 4 mm.

### III-2 Polarized target

The surroundings of the target and the inside view of the sample cell are shown schematically in Fig. 6. This target station for polarized neutron scattering has been developed by CERN (Niinikoski et al., 1976, 1982). The sample is immersed in a liquid  $^4\text{He}$  bath so as to be transparent to incident neutrons and cooled by thermal couple to the mixing chamber of the  $^3\text{He}/^4\text{He}$  dilution refrigerator. This refrigerator has 20 mM/s maximum circulation rate

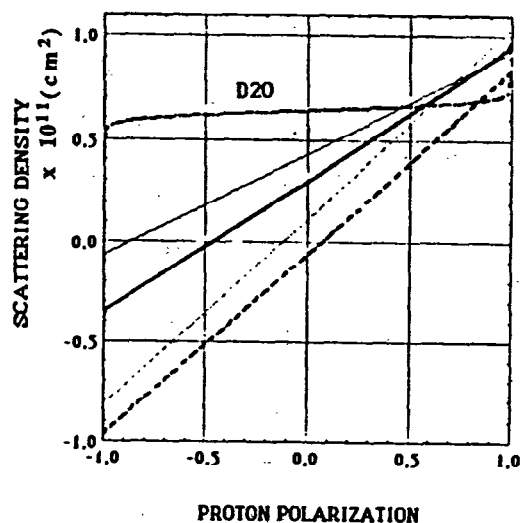


Fig. 5 Scattering length density vs. proton polarization: — protein, — DNA, --- lipid head, ---- lipid alkyl.

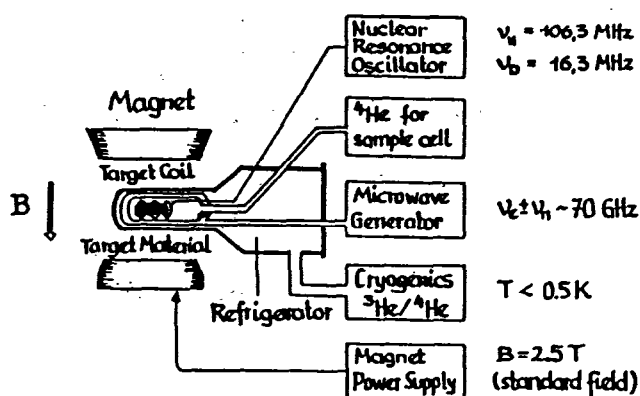
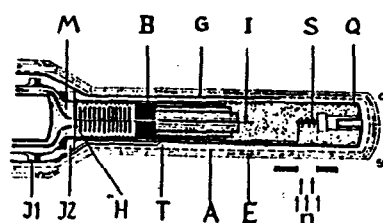


Fig. 6

Fig. 6 Schematic view of the target and its surroundings: mixing chamber M; heat exchanger B; sample S; quartz cell Q; inner vacuum chamber A; indium joints J1,J2; liquid  $^4\text{He}$  path I; microwave guide G; heat shield E (50 $\phi$ ).



of  $^3\text{He}$  and 1 mW cooling power at the sample position at  $T = 200$  mK. The procedure of the target cooling is as follows. The sample holder fixing the sample with a framework made of Teflon and fine ceramics is inserted in the quartz cell which is connected to the top of the refrigerator. After one hour pre-cooling by the use of liquid  $\text{N}_2$ , cooling with liquid  $^4\text{He}$  is started down to 20 K and continued with  $^4\text{He}$  gas exchange in the inner vacuum chamber. It takes four hour to reach 1K. Further cooling with more  $^3\text{He}$  circulation is still continued to reach 100 mK. Under 2.5 tesla magnetic field, the rate of the proton spin polarization by 69.1 GHz microwave irradiation is high enough, for instance, 20 %/min at the beginning. The maximum polarization of proton with water/glycerol solvent is 95 %.

The polarization of the target is monitored by the CW-NMR with a Q-meter circuit. Its absolute value is obtained by the calibration using the value of the proton spin polarization at 1k and 2.5 tesla. The accuracy of this calibration, mainly depending on that of the temperature measurements, is

better than 1 %. The depolarization of proton or deuteron is also done by irradiating appropriate modulated RF,  $v_H$  or  $v_D$ , through the NMR coil.

### III-3 Small-angle scattering spectrometer (SANS-1)

Fig. 7 shows the side view of SANS-1. Neutrons emerging from the reactor FRG-1 enter the H<sub>2</sub>-gas Cold Source with a flat bottle shape at 25 K through light water moderator and are reflected to the curved neutron guides by the beryllium reflector. At the end of the neutron guide (NG-1)  $10^8$  n/cm<sup>2</sup>/s is registered. The peak wavelength of Maxwell's distribution of neutrons is 6 Å. This neutron beam is monochromatized by the helical slot velocity selector with a band pass about 10 %. We have used the neutrons with the wavelength of 8.5 Å. After the monochromatization, the super mirror polarizer passes the neutrons with one spin direction through itself. Inside the movable neutron guide sections there are the collimator system and the Mezei type flat coil spin flipper for the inversion of the orientation of polarized neutrons. The magnetic guide field is applied for the polarized neutrons all the way from the polarizer to the sample. Under 2 m collimation condition,  $10^5$  polarized neutrons/cm<sup>2</sup>/s enter the sample. In the evacuated scattering chamber, the position sensitive area counter with 55 x 55 cm<sup>2</sup> sensitive area and 0.7 x 0.7 cm<sup>2</sup> effective pixel size can be moved from 0.7 m to 8 m distance from the sample.

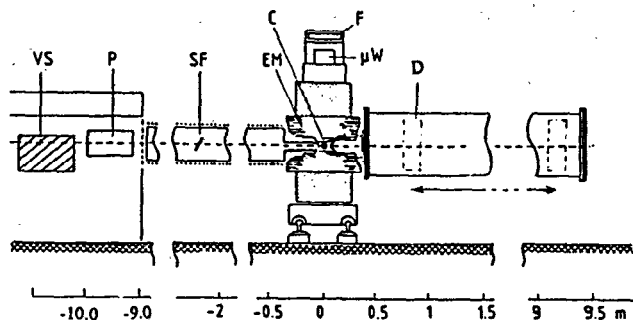


Fig. 7 The side view of SANS-1: velocity selector VS; polarizer P; spin flipper SF; electromagnet EM; nose of horizontal dilution refrigerator C; microwave generator  $\mu W$ ; microwave frequency counter F; movable area detector D. The length L of collimation is 2,3,5,7 & 9 m. The sample-detector distance is 0.7-8 m.

## IV. RESULTS AND DISCUSSIONS

Apoferritin, whose structure was well-defined by several authors (Stuhrmann et al., 1976), has been used as a standard sample to demonstrate the superiority of spin contrast variation over other methods (Stuhrmann, 1989). The polarized neutron scattering profiles at several proton polarizations are shown in Fig. 8. The scattering intensity of the apoferritin sample is minimized near  $P_H = 0.6$ , so-called at contrast matching point of apoferritin. According to the scheme in the preceding sections, each of the basic scattering functions is obtained as shown in Fig. 9. As those profiles coincide with one another, we can confirm that the homogeneous proton spin polarization has proceeded in fact. This result is very important for the feasibility of spin contrast variation in macromolecular research.

Using the same sample selective depolarization of protons and deuteron were carried out. The depolarization process was monitored by polarized

neutron scattering. The process of proton spin depolarization by RF irradiation  $\nu_H = 106.5$  MHz for 8 min. is shown in Fig. 10, which is explained by the change of spin-dependent scattering density  $\bar{\rho}_v$  (see in the figure caption). The experiments of the deuteron spin saturation with three samples: the preceding apoferritin solution, a 3 wt% bovine serum albumin solution and pure solvent (water glycerol mixture including 5 wt%  $H_2O$ ), were also done at 300 mK to measure the proton- deuteron thermal mixing time  $\tau_{HD}$ .  $\tau_{HD}$  depending on the proton concentration were 20 h, 50 h and 250 h for those samples, respectively.

The experiment of deuterated large ribosomal subunit was the first one in a series of the planned studies. In Fig. 10 three basic scattering functions are all different, in contrast to Fig. 9. This result is reasonable. Because large

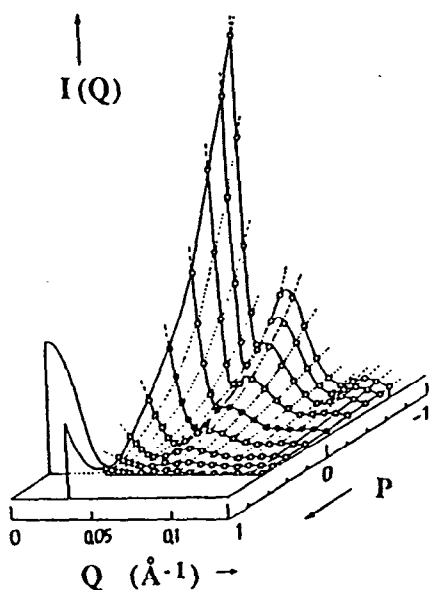


Fig. 8 (on the left side) Polarized neutron scattering  $I(Q)$  of apoferritin. Contrast minimum is at  $P=0.6$ .

Fig. 9 (on the right side) The basic scattering functions of apoferritin:  $I_u(Q)$  ○ ;  $I_{uv}(Q)$  ◐ ;  $I_v(Q)$  ● .

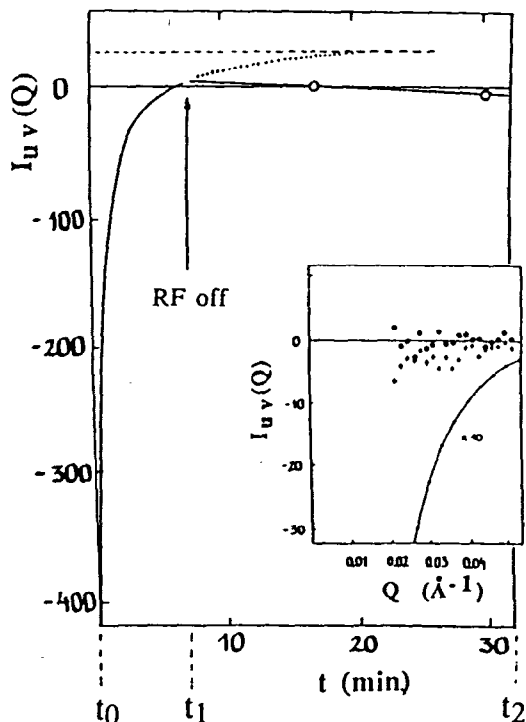
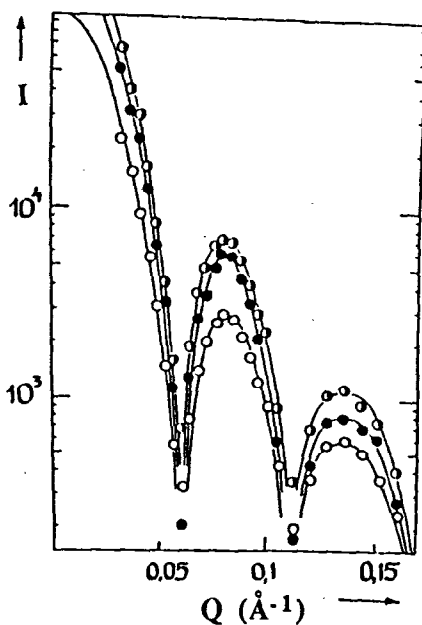


Fig. 10 Proton depolarization measurement of apoferritin. The sign of  $I_{uv}$  at each time is determined by the contrasts  $\bar{\rho}_u$  and  $\bar{\rho}_v$ : at  $t_0$  and  $t_2$ , ( $\bar{\rho}_u < 0$ ,  $\bar{\rho}_v > 0$ ); at  $t_1$ , ( $\bar{\rho}_u < 0$ ,  $\bar{\rho}_v < 0$ ). The insert shows the  $I_{uv}$  at 17' and 30'.

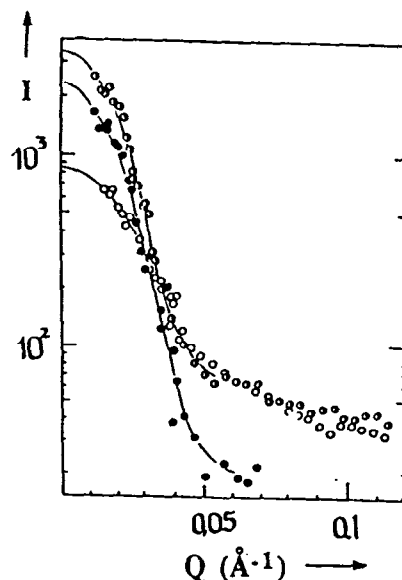


Fig. 11 The basic scattering functions of deuterated ribosomal subunit:  $I_u(Q)$  ○ ;  $I_{uv}(Q)$  ◐ ;  $I_v(Q)$  ● .



ribosomal subunit consists of two different species, i.e., protein and rRNA, the difference of the density of protons between these species results in unequal basic scattering function. More detailed results and discussions including these results will be done in another report (Knop et al.).

## References

- Abragam, A., & Goldman, M., Nuclear Magnetism: Order and Disorder, edited by J.A. Krumhansl, W. Marshall & D.A. Wilkinson, Oxford: Clarendon Press, (1982).
- Abragam, A., Bacchella, G.L., Coustham, J., Glättli, H., Fourmond, M., Malinowski, A., Meriel, P., Pinot, P. & Roubeau, P., *Journal de Physique* **44**,  
Boulin, C., Büldt, G., Dauvergne, F., Gabriel, A., Goerigk, G., Knop, W., Krumpolc, M., Munk, B., Nierhause, K.H., Niinikoski, T.O., Nowotny, V., Rieubland, M., Rijlart, A., Schärpf, O., Schink, H.-J., Wagner, R. & Stuhmann, H.B.,  
*Makromol. Chem., Macromol. Symp.* **15**, 19-49 (1988).
- Jin, Y. & Crichton, R.R., *FEBS Letts.* **215**, 41-46 (1987).
- Knop, W., Nierhaus, K.H., Nowotny, V., Niinikoski, T.O., Krumpolc, M., Rijlart, A., Schärpf, O., Schink, H.-J., Stuhmann, H.B. & Wagner, R., *Helv. Phys. Acta* **50**, 741-746 (1986).
- Knop, W., Schink, H.-J., Stuhmann, H.B., Wagner, R., Wenkow-Es-Souni, M., Schärpf, O. W., Krumpolc, M., Niinikoski, T.O., Rieubland, M. & Rijlart, A., *J. Appl Cryst.* **22**, 352-362 (1989).
- Knop, W., Hirai, M., Schink, H.-J., Stuhmann, H.B., Wagner, R., Zhao, J., Schärpf, O. W., Crichton, R.R., Krumpolc, M., Nierhaus, K.H., Niinikoski, T.O., & Rijlart, A., submitted to *J. Appl. Cryst.*
- Krumpolc, M., Rocek, J., *Inorganic Chemistry* **24**, 617-621 (1985)
- Niinikoski, T.O. & Udo, F., *Nucl. Instrum. Methods* **134**, 219-233 (1976).
- Niinikoski, T.O., & Rijlart, A., *Nucl. Instrum. Methods* **199**, 485-489 (1982).
- Stuhmann, H.B., Schärpf, O. W., Krumpolc, M., Niinikoski, T.O., Rieubland, M. & Rijlart, A., *Eur. Biophys. J.* **14**, 1-6 (1986).
- Stuhmann, H.B., *Physica B* **156** & **157**, 444-451 (1989).